Full Paper Wiley Online Library ELECTROANALYSIS

DOI: 10.1002/elan.201400726

Faradic Peaks Enhanced by Carbon Nanotubes in Microsomal Cytochrome P450 Electrodes

C. Baj-Rossi,*[a] C. Müller,[b, c] U. von Mandach,[c] G. De Micheli,[a] and S. Carrara[a]

Abstract: In this work we present an investigation on the behavior of microsomes containing human cytochrome P450 in cyclic voltammetry for drug detection. The microsomes are adsorbed on the surface of multi-walled carbon nanotubes by drop-casting. We demonstrate that the hydrophobic and highly electroactive surface of multi-walled carbon nanotubes enables to distinguish more clearly the contributions in reduction peak current attributed to the enzymatic components of microsomes. Voltammetric measurements were performed under several experimental conditions with two cytochrome P450-isoforms, 1A2 and 3A4. We show that the reduction current for the component of cytochrome P450-microsome linearly increases in the presence of a substrate.

Keywords: Cytochrome P450 · Drugs · Electrochemical biosensors · Carbon nanotubes · Purified cytochrome P450

1 Introduction

The increasing needs of personalized therapies have recently stimulated impressive advances in research and development of portable point-of-care biosensors for real-time monitoring as well as biosensors for drug development [1,2].

Enzymatic amperometric biosensors based on the enzyme family *cytochrome P450* (CYP) have drawn increasing attention because CYP is a monooxygenase enzyme primarily involved in the metabolism of bioactive metabolites and hydrophobic xenobiotics such as drugs, environmental pollutants and steroids [3]. The 3D structure of the enzyme is illustrated in Scheme 1A.

CYP catalyses the monooxygenase reaction, a two-electron reaction where the electrocatalytic transformation of a substrate is coupled to the electrocatalytic reduction of oxygen, according to the general equation:

$$RH + O_2 + 2e^- + 2H^+ \rightarrow ROH + H_2O$$

A substrate (RH) is hydroxylated (ROH) through the insertion of one oxygen atom into the substrate, while the second atom of oxygen is reduced to water [4]. The two electrons necessary for the monooxygenation are provided by the redox reaction of the heme group in the active site of the CYP (Scheme 1A), which is *in-vivo* activated through electron transfer from its redox partners: two electrons derived from NAD(P)H are transferred to the CYP active site via the electron transport protein, *cytochrome P450 reductase* (CPR) [6]. The direct immobilization of CYP on an electrode overcomes the need for NAD(P)H and CPR, as the electrons needed for the redox reaction of the heme group are directly supplied by the electrode [4,5,7,8].

Another approach is the electrode functionalization with *microsomes containing both CYP and CPR* (msCYPs). msCYPs are commonly used in the industry for drug development [2]. As reported in [2,7,9], the discovery that microsomes are as effective as recombinant CYPs in enabling direct electrochemistry on electrodes promoted an increasing interest in biosensors based on microsomes-CYP, as the production of microsomes is cheaper than recombinant CYPs. In a previous study [9] msCYPs were immobilized on a polycation-coated electrode and the authors proved that the direct electron transfer occurred according to the natural electron transfer path (electrode→CPR→CYP). Moreover, a more recent work [10] proved that, in presence of a substrate, the amount of metabolite formation in the microsomes containing the reductase was almost double respect to what obtained with CYP alone. The authors concluded that the electron transfer from the electrode to the CPR and then to the CYP is a more efficient pathway than the direct electron supply to the CYP. In this work the authors also showed that a hydrophobic electrode surface facilitates the immobilization of msCYP, because of the presence of hydrophobic regions in the surface structure of CYP, CPR and the lipids that compose the microsome.

With cyclic voltammetry (CV) or other electro-analytical techniques, it is possible to apply a potential to the immobilized CYP and record the current that is produced. This current can be attributed to the reduction of

[a] C. Baj-Rossi, G. De Micheli, S. Carrara
Laboratory of Integrated Systems, EPFL – École Polytechnique Fédérale de Lausanne
1015 Lausanne, Switzerland
*e-mail: camilla.baj-rossi@epfl.ch

[b] C. Müller
Obstetrics Department, University Hospital of Zürich
8091 Zürich, Switzerland

[c] C. Müller, U. von Mandach
Inorganic Chemistry Laboratory, ETHZ Zürich
8093 Zürich, Switzerland

Supporting Information for this article is available on the WWW under http://dx.doi.org/10.1002/elan.201400726

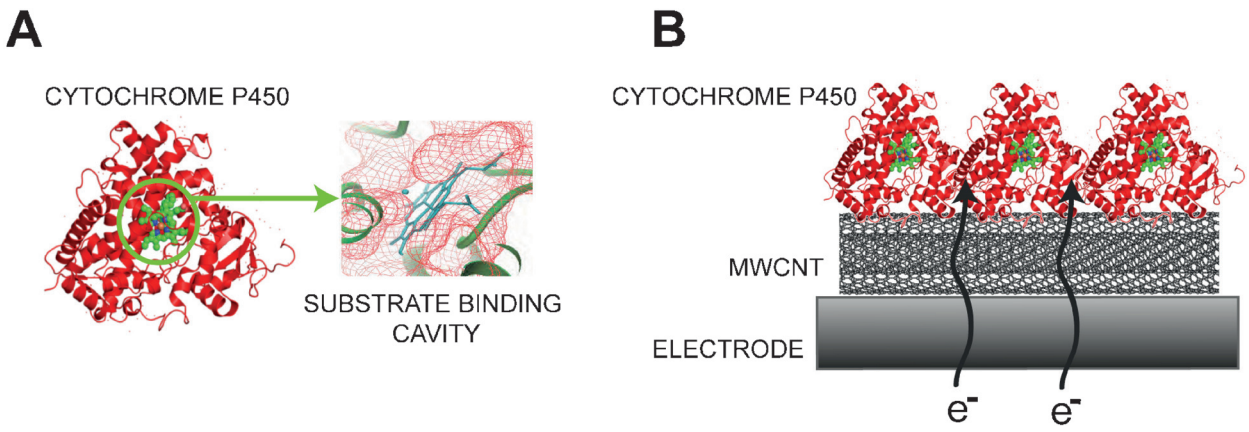

Scheme 1. A) Structure of CYP (the isoform 1A2, from PDBe Protein Data Bank Europe), with a closer view of the heme group in the substrate-binding cavity. B) Scheme of the electrode functionalization with drop-cast MWCNTs and msCYP (here generically named "cytochrome P450").

the active site of the enzyme and it will increase in presence of a CYP substrate, e.g. a drug, or oxygen [6,11]. The oxidation/reduction of the heme group of CYP results in CV peaks at positions that can vary according to the way the enzyme is immobilized and the presence of a nanostructure, or the electrode material [5,12], as reported in many works of biosensors based on CYP1A2 and CYP3A4 [3,5,8,9,13,14,15,16,17,18,19,20,21,22]. From this analysis, it emerges that for each electrode modification and CYP preparation it is necessary to identify the voltammetric peaks due to the reduction of CYP.

We report in this paper an enhanced electron transfer in CV from the electrode to the microsome containing CYP and CPR, by creating a hydrophobic and highly electroactive surface with drop-cast multiwalled carbon nanotubes (MWCNTs) on a screen-printed electrode (SPE). Scheme 1B shows the scheme for the electrode functionalization. The two arrows represent the electron transfer (e^-) between the electrode and the protein. The enhanced electron transfer to the heme-enzyme results in a higher reduction current that enables to distinguish more clearly the contributions in current attributed to the redaction peaks of the microsome components, CYP and CPR. Voltammetric measurements were performed under several experimental conditions with microsomes of two CYP-isoforms, CYP1A2 and CYP3A4. We also immobilized on a MWCNT-SPE purified CYP3A4 (without CPR) and purified CPR (without CYP3A4) and confirmed by CV the position of the reduction peaks of the two components.

Moreover, we confirm that the reduction current for the CYP component of the msCYP increases in the presence of a substrate (i.e. a drug) as has previously been shown in other studies involving microsomal CYPs [9,10].

2 Experimental

2.1 Reagents and Chemicals

MWCNTs (~10 nm diameter and ~1–2 μm length) with 5% COOH groups content were purchased as a powder (90% purity) from DropSens.

Microsome containing cytochrome P4501A2 (msCYP1A2) and microsome containing cytochrome P4503A4 (msCYP3A4) were purchased from Sigma-Aldrich (St. Gallen, Switzerland) as isozyme microsomes with recombinant human CYP1A2 (or CYP3A4), recombinant rabbit NADPH-P450 reductase, and cytochrome b_5 (0.5 nmole of cytochrome P450 isozyme in 100 mM potassium phosphate, pH 7.4.) and used as received. All experiments were carried out in a 100 mM phosphate buffered saline solution (PBS, pH 7.4) as supporting electrolyte.

The drugs Naproxen [(*S*)-6-methoxy-α-methyl-2- naphthalene acetic acid] (NAP) and Ifosfamide (IFO), purchased as a powder from Sigma-Aldrich, were dissolved in chromatography grade methanol and milliQ water respectively.

CHAPS 3-[(3-cholamidopropyl)-dimethylammonio]-1-propansulfonat was purchased from Applichem GmbH (Darmstadt, Germany). HisPur nickel nitrilotriacetic acid (Ni-NTA) beads were ordered from Thermo Fisher Scientific (Waltham, USA). CM macro-prep ion exchange support was ordered from Biorad (Hercules, USA). E. coli HMS 174 (DE3) was ordered from Merck (Darmstadt, Germany). The diethylaminoethanol (DEAE) sepharose fast flow and adenosine 2′,5′-diphosphate agarose supports were both ordered from Sigma-Aldrich (St. Louis, USA). DOPC (1,2-di-(9Z-octadecenoyl)-*sn*-glycero-3-phosphocholine) was purchased from Avanti Polar Lipids (Alabaster, USA).

EDTA (ethylenediaminetetraacetic acid) and DTT (dithiothreitol) were purchased from Sigma-Aldrich. Hydrogen peroxide (30% vol) was purchased from Sigma-Al-

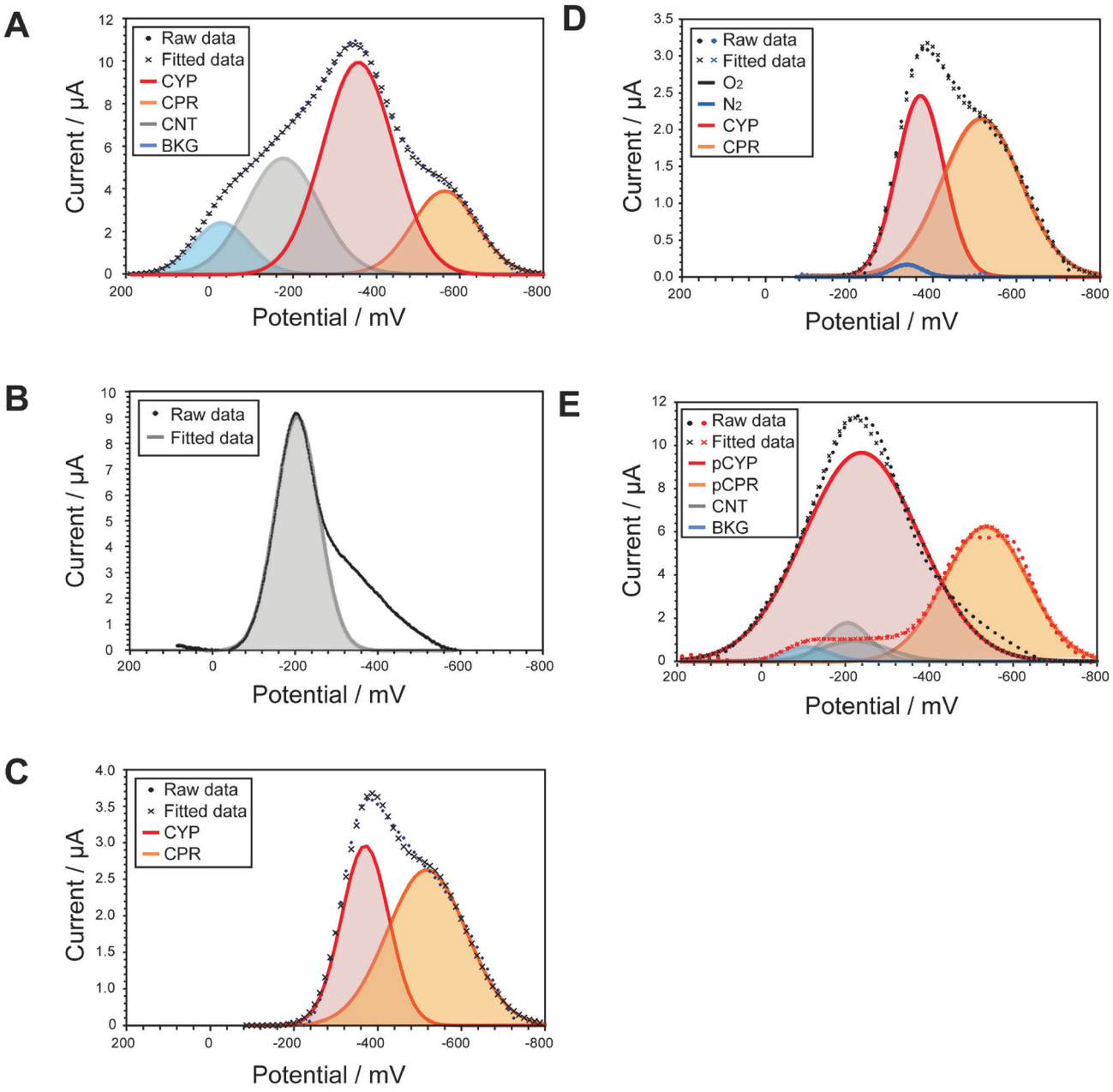

Fig. 1. Reduction current peaks from CV after background subtraction, for msCYP3A4 on a MWCNT-modified SPE (A), for a MWCNT-modified SPE without protein (B), for msCYP3A4 on a bare-SPE (C), for msCYP3A4 on a bare-SPE in the presence (black points) and absence (blue points) of oxygen (D) and for the purified proteins (pCYP3A4 and pCPR) on MWCNT-modified SPEs (E). Symbols used: cytochrome P450 (CYP), cytochrome P450 reductase (CPR), carbon-nanotubes (CNT), background (BKG).

drich and diluted to the desired concentration. HEPES (4-(2-hydroxyethyl) piperazine-1-ethane sulfonic acid) was purchased from Thermo Fisher Scientific (Waltham, USA).

2.2 Expression and Purification of CYP3A4 and Cytochrome P450 Reductase

The construct pSE3A4 expressing human CYP3A4 was described previously [23,24]. It contains 4 histidine residues at the C terminus of the CYP3A4 coding sequence. Briefly, freshly transformed *E.coli* Topp3 cells were induced with 0.5 mM isopropyl β-D-1-thiogalactopyranosid (IPTG) and the CYP3A4 construct expressed for 48–72 hours before cells were lysed by sonication and expression levels quantified by reduced carbon monoxide binding [25]. Solubilized membranes containing the enzyme were purified via nickel-affinity chromatography using Ni-NTA beads and anion exchange chromatography using CM macro-prep ion exchange support. Human P450 oxidoreductase from the construct CPR [26] was expressed in E. coli HMS 174 (DE3) and captured on an

anion exchange chromatography support (DEAE sepharose fast flow) and polished on an adenosine 2′,5′-diphosphate agarose support.

The purity of the enzymes was analyzed via SDS-gel electrophoresis and absorption spectroscopy. The recorded spectra were compared to available standard spectra of purified CYP3A4 (pCYP3A4) and purified CPR (pCPR) and quantified using spectralab software [27]. The concentration of pCYP3A4 (77 μM) and pCPR (101 μM) were reduced to 20 μM by diluting the protein preparation in a 50 mM (pH 7.4) potassium phosphate buffer containing 0.5 mM EDTA.

The reconstituted systems (recCYP3A4 and recCPR with cytochrome b_5) were prepared by diluting the following reagents in our buffer (100 mM HEPES pH7.4, 1mM EDTA, 1 mM DTT 10% glycerol, 150 mM KCl): CYP3A4 and CPR to a final concentration of 20 μM each, cytochrome b_5 to a final concentration of 10 μM, CHAPS to 7.7 mM, DOPC to 0.15 mM. The reconstituted enzyme was stored at −80 °C when not directly used.

2.3 Preparation of msCYP/MWCNT Electrodes

The biosensors were prepared using commercial carbon paste SPEs (model DRP-C110, DropSens, Spain) consisting of a graphite working electrode with an active area of 12.56 mm^2, a graphite counter electrode and an Ag|AgCl reference electrode. A 1-mg/mL solution of MWCNTs, prepared in chloroform, was sonicated for 30 min to obtain a homogeneous suspension [28]. The procedure used to drop-cast MWCNTs and the enzyme solution on SPEs, is described in Reference [18]. After the protein deposition, the electrodes were stored at 4 °C overnight to promote a homogeneous protein adsorption on the CNT-nanostructure.

2.4 Apparatus

Electrochemical measurements were performed using an Autolab electrochemical workstation (Metrohm, Switzerland). The scanning electron micrographs (SEM) were acquired using a Philips/FEI XL-30F microscope (Philips, Eindhoven, The Netherlands). The scanning electron microscope was operated in 1.5–4.2 mm ultra-high resolution mode (UHR). The resolution was 2.5 nm at 1 kV.

2.4 Electrochemical Measurements

The electrochemical response of the biosensor was investigated by CV at room temperature under aerobic and anaerobic conditions by applying a potential sweep between −800 and +300 mV vs. Ag|AgCl at a scan rate of 20 mV/s. For experiments carried out under anaerobic conditions, the 100 mM PBS solution was bubbled with N_2 for 45 minutes before measurements in a sealed electrochemical cell. During the measurements, N_2 was continuously fluxed on the solution surface in order to avoid oxygen contamination and not to affect the measurements.

For the sensor calibration to NAP and IFO, drug samples were added in increasing concentrations. The electrode was covered with 100 μL of 100 mM PBS (pH 7.4) and drug samples were added in 1 μL drops. Sensitivity per unit area was calculated from the peak current that was estimated according to the procedure reported by [30,31]. The limit of detection (LOD) was computed as three times the signal-to-noise ratio according to the expression [32,33] $LOD = k\delta i/S$, where δi is the standard deviation of the blank measurements, S is the sensitivity, and k is a parameter accounting for the confidence level ($k = 1$, 2, or 3 corresponds to 68.2%, 95.4%, or 99.6% of confidence, respectively).

3 Results and Discussion

3.1 Identification of the Cathodic Reduction Peaks for msCYP

To characterize more precisely the peaks obtained for microsomes adsorbed on MWCNTs, an analysis of the reduction peaks obtained in CV was carried out under several experimental conditions: with bare or MWCNT-modified electrodes, in aerobic/anaerobic conditions, with two CYP isoform (msCYP1A2 and msCYP3A4) and with purified CYP3A4.

3.1.1 Reduction Peaks of msCYP3A4 on MWCNT-Modified or Bare Electrode

Figure 1 shows the reduction current peaks in the potential window +200/−800 mV for five cases: for msCYP3A4 on a MWCNT-modified SPE (A), for a MWCNT-modified SPE without protein (B), for msCYP3A4 on a bare-SPE (C), for msCYP3A4 on a bare-SPE in the presence (black points) and absence (red points) of oxygen (D) and for the purified proteins (pCYP and pCPR) on MWCNT-modified SPEs (E).

The resolution of peak overlapping with mathematical functions, is a procedure well known in literature [50,51], and can be used to visualize the faradic current generated by the various biosensor components. The basic functions used for the decomposition are the Guassian, the Hyperbolic cosine and the Cauchy function [52]. More complex functions are usually based on modifications or combinations of these three.

In order to visualize the individual contributes of CNT, CYP and CPR, we normalized the reduction current between +200 and −800 mV to the baseline obtained with the automatic peak recognition software, and we used the Gaussian functions to describe the different faradic contributes. The peak position of each gaussian was initially cantered according to the data obtained from literature and then optimized with the fitting. The y values of each Gaussian where then summed up, while height and ampli-

tude where fitted to the current profile obtained from the raw data [29].

In Figure 1 the Gaussian curves in subfigures (A-B-C-D-E) share the same color code in order to display similarities and differences between peaks. Figure 1A shows the background-subtracted reduction peaks from the CV for msCYP3A4 adsorbed on a MWCNT-modified-SPE. We observe four different peaks in the reduction region: at −540 mV, at −360 mV, at around −200 mV and at −50 mV. Figure 1B shows the background-subtracted reduction peaks from the CV for a MWCNT-modified SPE without protein. Figure 1C reports the background-subtracted reduction peaks for msCYP3A4 on a bare-SPE. For msCYP3A4 on bare electrodes only two reduction peaks were observed and fitted with two Gaussian functions: at −540 mV and −360 mV.

With both bare and MWCNT-modified electrodes, we observed two reduction peaks in the region −300/−600 mV: one reduction peak at −360 mV and one at −540 mV. The reduction peak at −360 mV is due to the electron transfers to CYP, while the peak at −540 mV can be attributed to the reduction of CPR. Positions of peak potentials are in good agreement with the peak positions reported in recent studies on microsomes containing CYP and CPR [9,10], where the authors showed that in CV both CYP and CPR give a contribution in the form of reduction peaks. In particular, the authors in [10] showed for microsomal CYP3A4 a CYP reduction peak at −380 mV and a CPR reduction peak at −420 mV. The potential peak for CPR was confirmed in other individual electrochemical studies [34].

We attributed the peak at around −200 mV to the reduction of the carboxyl groups of carbon nanotubes [35] as shown in Fig.1B (SPE is modified with MWCNTs, without proteins). In Figure 1A, the CNT-peak (gray line) at −200 mV displays a lower current, because the microsomal components cover the MWCNTs. The peak at −50 mV (labeled as "BKG") can be attributable to the reduction of other microsomal components [36].

This peak is also present for the msCYP on a bare-SPE, but it is not present anymore after background subtraction (Figure 1C). From Figure 1, it is evident that the presence of carbon nanotubes increases the reduction current for the microsomal component CYP: the CYP reduction peak current value is significantly larger than the CPR peak, for the MWCNT-SPE (Figure 1A), respect to the bare SPE (Figure 1C). This carbon nanotube effect in enhancing the reduction current will be discussed in Section 3.2.

3.1.2 Reduction Peaks of msCYP3A4 in Aerobic/Anaerobic Conditions

To characterize more precisely the peaks obtained for microsomes adsorbed on MWCNTs, voltammetric responses of msCYP3A4 were studied in substrate-free PBS in aerobic/anaerobic conditions. In agreement with previous findings [3,10,11], we expected a decrease in the cathodic current peak of the microsomal component CYP upon the depletion of oxygen from the solution.

In Figure S1 (Supporting Information) the whole voltammograms for msCYP3A4 on bare-SPE (A) and a MWCNT-SPE (B) are reported, in aerobic and anaerobic conditions. In absence of O_2 we can observe the oxidation peak for the microsomal component CYP that otherwise would be completely attenuated in the presence of O_2 in the solution [5]. Figure S2 (Supporting Information) shows the background-subtracted oxidation and reduction peaks for msCYP3A4 on a bare SPE in anaerobic conditions. This evaluation of the CV peaks revealed that the oxidation peak current is slightly smaller than the corresponding reduction peak. This can be ascribed to the presence of traces of oxygen due to an imperfect sealing of the buffered solution and to the low scan rate (20 mV/s) that makes the oxidation peak more difficult to observe [11].

Figure 1D shows the background-subtracted reduction peaks from the CV for msCYP3A4 on a bare-SPE in an N_2-saturated buffered solution (blue dots, labeled as "N_2") and in aerobic conditions (black dots, labeled as "O_2"). Figure 1D shows a clear decrease of the cathodic current at −360 mV when oxygen is depleted from the solution, and a subsequent increase of cathodic current back to the initial value when aerobic conditions are established again (black dots, labeled as "O_2"). The increase of the cathodic current in presence of oxygen is characteristic for the electrochemical response of heme-containing proteins such as CYP [10,11], hemoglobin [37] and myoglobin [35]. In conclusion we confirm that the cathodic peak at −360 mV is ascribed to the reduction of the microsomal component CYP.

3.1.3 Purified CYP3A4 and CPR

To further confirm that the peak at −360 mV can be attributed to the reduction of the microsomal component CYP, voltammetric measurements on MWCNT-SPE were carried out with two preparations of purified proteins: pCYP3A4 (without CPR) and pCPR (without CYP). Figure 1E shows the background-subtracted reduction peaks from the CV for the purified proteins (pCYP and pCPR) on MWCNT-modified SPEs. pCPR (red dots) gives a well-defined reduction peak at −550 mV, while the pCYP3A4 (black dots) gives a reduction peak at −240 mV. It is positively shifted by 100 mV with respect to the msCYP3A4, thus making it overlapping with the reduction peak of CNTs. This may be due to the absence of other microsomal components (CPR, lipids). However, the potential of the reduction peak of pCYP3A4 is in good agreement with previous studies on purified proteins [19,21].

Voltammetric experiments on MWCNT-SPEs were also conducted with two preparations of reconstituted proteins: recCYP3A4 (without CPR) and recCPR (without CYP3A4) and the results are reported in Figure S3 (Supporting Information). With recCYP3A4 (black dots) we

can identify the peak at −380 mV similar to the peaks found for msCYP3A4 on MWCNT-SPE (Figure 1A). The peak at −540 mV is not present while it is clearly visible in the reduction region of the recCPR (red dots), thus confirming the previous results.

3.1.4 Reduction Peaks of msCYP1A2

We performed similar experiments also with msCYP1A2, as illustrated in Figure S4 in the Supporting Information. The only difference is that the microsome peaks are positively shifted by 20 mV: the CYP peak is centered at −380 mV (red line) and the CPR peak at −560 mV (orange line).

To further confirm that the cathodic peak at −380 mV can be attributed to the reduction of the heme protein i.e. the CYP component of microsome, CV was performed in the presence of increasing concentrations of hydrogen peroxide (H_2O_2), since it has been reported that proteins containing a heme group, such as CYP [9,10], hemoglobin [35,37], myoglobin [35] and horseradish peroxidase [38], can catalyze the reduction of H_2O_2.

In all the cited studies a large cathodic current for the reduction of H_2O_2 appears at the reduction potential of the heme protein, while the anodic peak disappears completely. With our msCYP we observed the same behavior: Figure S5 (Supporting Information) shows the reduction peaks after the background subtraction for the msCYP1A2-bare SPE in presence of H_2O_2 at different concentrations (1 and 5 mM). When H_2O_2 is added, the msCYP1A2-bare SPE shows a large reduction peak at around −380 mV that increases with the concentration of H_2O_2 in solution. With the same H_2O_2 concentrations we observe a smaller increase in reduction current for a bare-SPE, without the enzyme.

3.2 Enhancement of Reduction Current of Microsomal CYP with MWCNTs on SPE

To better understand the improvement in the electrochemical reactivity of the protein when it is adsorbed on MWCNTs, we estimated the surface concentration of the electroactive CYP1A2 and CYP3A4 on the electrode, Γ (in mol/cm^2). Γ can be estimated using the equation $\Gamma = Q/nFA$, where Q is the charge consumed (in C), obtained from integrating the cathodic peak area in CV after the background correction (divided by the scan rate), n is the number of electrons exchanged in the redox ($n=1$) [11], A the electrode area (0.1256 cm^2) and F the Faraday constant (in C mol^{-1}) [39].

The values of Γ for CYP1A2 and CYP3A4 on bare and MWCNT-coated electrodes are reported in Table 1. The values of Γ were calculated for a scan rate of 20 mV/s. The total amount of proteins drop-cast on the electrode is 3.98 nmol/cm^2 (estimation, from vials of ~ 0.5 nmol, on electrodes with area equal to 0.1256 cm^2). From the data presented in Table 1, only a part of the CYP on the electrode surface undergoes the direct electron transfer reaction. The fraction of electroactive CYP over the total adsorbed protein on the MWCNT-modified electrode is 80% for CYP1A2 and 83% for CYP3A4. These values are higher than the 54.7% obtained for hemoglobin immobilized on a Nafion-CNT electrode [37], and other heme-containing proteins immobilized in surfactant or polymers [40], indicating that MWCNTs are very effective in promoting the direct electron transfer of CYP, as has already been found in [35,37]. This is also confirmed by the smaller fractions of electroactive msCYP obtained when bare electrodes are used instead of the MWCNT-coated electrodes, which is 27% for CYP1A2 and 61% for CYP3A4. We observed a large variation in the fraction of electroactive CYP on bare electrode due to the unstable immobilization of the protein on the electrode surface.

MWCNTs have been recognized as promising nanomaterials for facilitating electron transfer in biosensing [41], because of their electrical and electrochemical properties: small size with large surface area, high conductivity, high chemical stability and sensitivity [42,43]. MWCNTs enhance the electrochemical reactivity of proteins or enzymes probably due to the presence of some oxygen-contained groups (e.g. carboxyl groups) [37] on the carbon-nanotube surface.

Moreover, MWCNTs create a hydrophobic and highly electroactive surface when they are drop-cast on electrodes, as already shown in our previous works [28,31].

We obtained higher values of Γ than for bare-SPE, due to the increase in electroactive area of the electrode due to MWCNTs that creates a three-dimensional porous structure with a larger effective surface area available for protein deposition as shown in the SEM of Figure 2. Figure 2A shows the SEM of the surface of a graphite SPE after the deposition of 30 μg of MWCNTs, acquired with an 8000× magnification, where the three-dimensional structure of the MWCNT agglomerate is shown. Figure 2B shows a SEM acquired at the same surface of MWCNT-SPE at higher magnification (80 000×). The enhancement of the CYP electrochemical reactivity after adsorption on MWCNTs results in higher peak currents for the microsomal component CYP as shown in Figure 1.

Table 1. Γ of electroactive enzyme and percentage relative to the total amount of deposited protein.

CYP isoform	Γ of electroactive CYP (nmol/cm^2)		Electroactive protein (%)	
	BARE SPE	MWCNT-SPE	BARE SPE	MWCNT-SPE
CYP1A2	1.07 ± 0.04	3.2 ± 0.1	27	80
CYP3A4	2.42 ± 0.09	3.77 ± 0.15	61	83

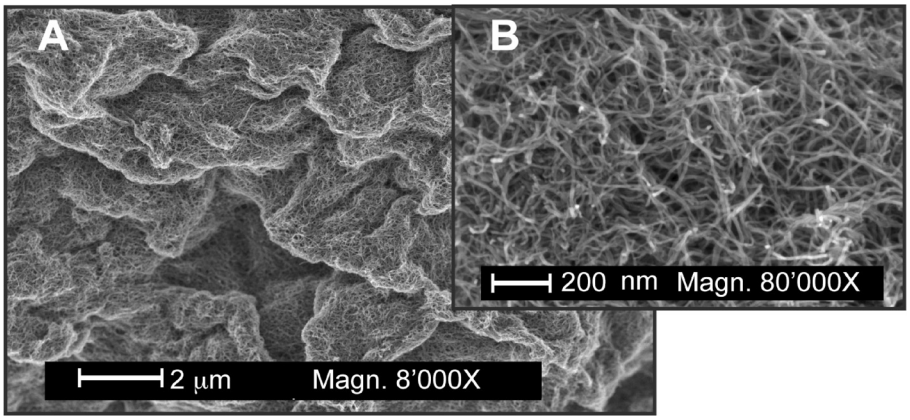

Fig. 2. Comparison of typical SEM of the surface of a graphite SPE after the deposition of 30 μg of MWCNTs, acquired with an 8000X magnification (A) and with an 80000 magnification (B).

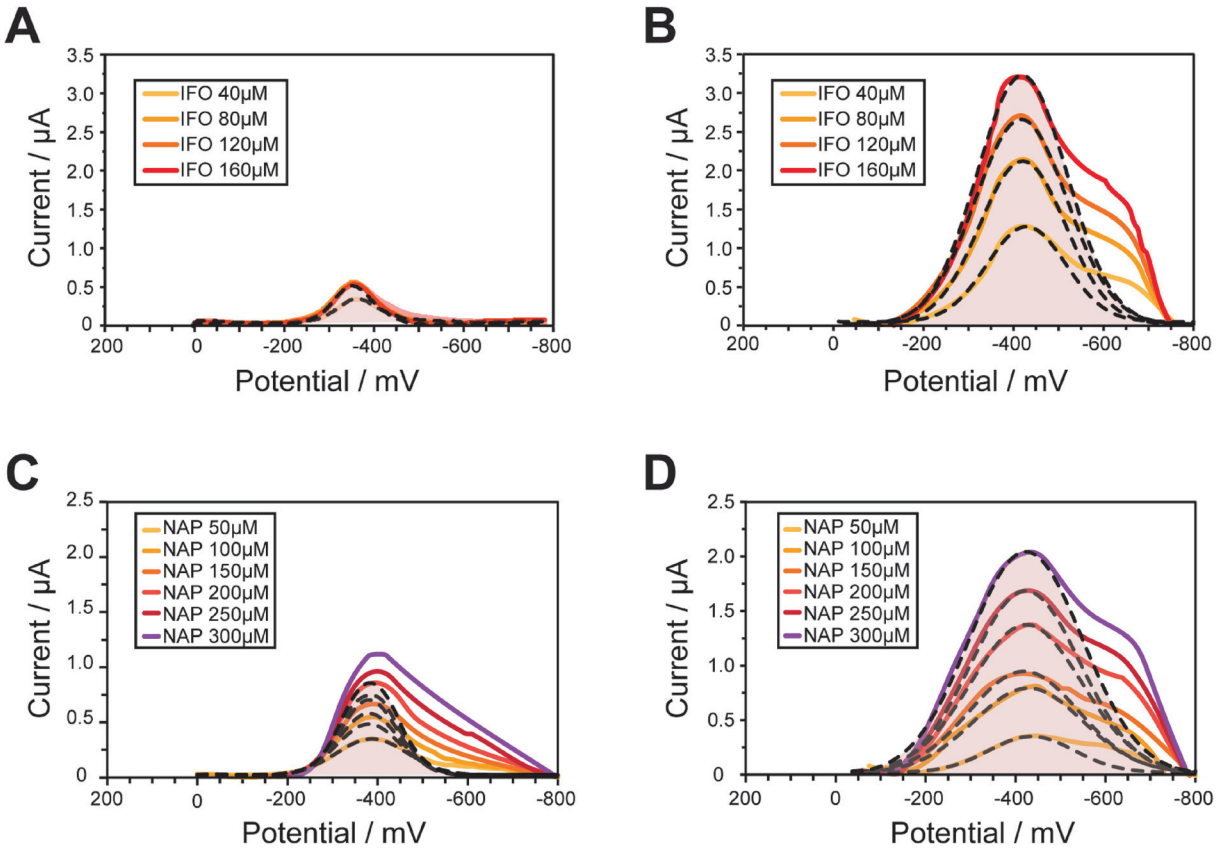

Fig. 3. Reduction current peaks from CV after background subtraction for a msCYP3A4-bare SPE (A) and for a msCYP3A4/MWCNT-SPE (B) at increasing concentration of IFO; Reduction current peaks from CV after background subtraction for a msCYP1A2-bare SPE (C) and a msCYP1A2/MWCNT-SPE (D) for increasing concentrations of NAP.

The MWCNT-enhancement in msCYP reduction current has been shown with a comparative experiment for msCYP/MWCNT-SPE and msCYP-bare SPE in presence of increasing concentrations of a drug. The measured drugs are, for CYP1A2, Naproxen (NAP), an anti-inflammatory agent with analgesic and antipyretic properties [44], and, for CYP3A4, Ifosfamide (IFO), a widely used anti-cancer drug [45]. Both NAP and IFO were measured in therapeutic concentrations: 10–160 μM for IFO [46] and 9–300 μM for NAP [47].

Figure 3 shows peak reduction current values obtained for msCYP3A4-bare SPEs (Figure 3A), and for msCYP3A4/MWCNT-SPEs (Figure 3B) for increasing concentrations of IFO. Figure 3C and Figure 3D show the peak reduction current values for msCYP1A2-bare SPE and msCYP1A2/MWCNT-SPE respectively, in the pres-

Table 2. Comparison in Sensitivity and LOD between SPEs functionalized with MWCNTs and bare SPEs for msCYP1A2 for NAP detection and msCYP3A4 for IFO detection.

msCYP-drug	Sensitivity (μA/mM cm^2)		Limit of detection (μM)	
	BARE SPE	MWCNT-SPE	BARE SPE	MWCNT-SPE
CYP1A2	16±2	54±2	64±32	16±1 [18]
CYP3A4	20±131	104±24	22±160	4±2

ence of increasing concentrations of NAP. In the *y*-dimension, reduction currents obtained from CV are shown after background subtraction and the normalization with respect to the voltammogram obtained in PBS in the absence of drug. The normalization was done in order to show only peaks that were increasing after the addition of drug. Figure S6 (Supporting Information) shows the whole voltammogram for the msCYP1A2/MWCNT-SPE sensor at different NAP concentrations. The addition of a substrate, e.g. a drug, results in a further increase of the CYP reduction current proportional to the substrate concentration [11]. This phenomenon has been verified for a number of different CYPs immobilized onto electrodes, such as CYP2C9 [12], CYP2B4 [11,17], CYP3A4 [19], CYP2B6 [48], CYP2D6 [49], and CYP1A2 [14,16]. This was verified, in our recent work, for msCYP1A2 in the presence of Naproxen [18].

As we expected, the reduction peak current of the microsome-CYP component shown in Figure 3 (highlighted in red) linearly increases with drug concentration. The increase in current is more evident with msCYPs adsorbed to a MWCNT-modified SPE, than to a bare-SPE. Also the peak of the CPR component shows a slight increase, but less significant.

Control experiments were performed with methanol and milliQ instead of drug and we could confirm that the voltammograms for msCYP/MWCNT-SPE did not show any significant change (data not shown).

From the peak currents at different drug concentrations reported in Fig.3, we obtained the calibration curves. Table 2 reports an overview of sensitivity and limit of detection (*LOD*) obtained from the calibration curves: for NAP detection with msCYP1A2 and for IFO detection with msCYP3A4.

As shown in Table 2, with msCYP-bare SPEs there is generally lower sensitivity, higher data variability and noise, resulting in a lower linearity, higher uncertainty in the estimation of LOD and higher LOD, with respect to the msCYP/MWCNT-SPE sensors. This shows that MWCNTs greatly enhance electron transfer between electrode and msCYP.

In conclusion, this comparative study shows that MWCNTs improve the sensor performance in both studied microsomal systems (the CYP isoforms 1A2 and 3A4).

Both msCYP1A2 and msCYP3A4 on a MWCNT-SPE exhibited a wide linear range and a sensitivity acceptable for detection of NAP and IFO respectively. Sensitivity and LOD values proved that drug detection in the therapeutic range has been successfully achieved due to the synergistic effect of msCYP and MWCNTs in enhancing the reduction current.

4 Conclusions

In this work, we demonstrated that: 1) with voltammetric measurements in several experimental conditions we can clearly identify the reduction peak for each CYP component of microsomes, which is essential to measure drug concentrations; 2) with MWCNTs we have more electroactive enzyme adsorbed on the electrode as compared to a bare electrode; 3) this results in a better definition of all peaks obtained in voltammetry that refer to different microsomal components, also in a complex system such as microsomes containing CYP and CPR; 4) the enhancement of the reduction current of msCYP by carbon nanotubes results in an improvement in the sensing performance of drugs.

Moreover, we proved that the hydrophobic surface created by MWCNTs can actively drive the electrochemical detection of drugs more efficiently than the unmodified SPE. In conclusion, MWCNTs could represent an ideal electrode modification to greatly enhance the sensor performance by improving the electron transfer to the protein and by retaining the activity of CYP toward drugs.

Acknowledgements

The SNF Sinergia Project, Code CRSII2_147694/1 'Innovative Enabling Micro-Nano-Bio-technologies for Implantable Systems in Molecular Medicine and Personalized Therapy – (Project prolongation)' financially supported this research. *Patricia L. Bounds* is acknowledged for her help with the protein purification. *Federico Angiolini* and *Andrea Cavallini* are acknowledged for the proofreading of the manuscript.

References

[1] P. D'Orazio, *Clin. Chim. Acta* **2011**, *412*, 1749–1761.
[2] E. Schneider, D. S. Clark, *Biosens. Bioelectron.* **2013**, *39*, 1–13.
[3] N. R. Hendricks, T. T. Waryo, O. Arotiba, N. Jahed, P. G. Baker, E. I. Iwuoha, *Electrochim. Acta* **2009**, *54*, 1925–1931.
[4] S. J. Sadeghi, A. Fantuzzi, G. Gilardi, *Biochim. Biophys. Acta* **2011**, *1814*, 237–248.
[5] N. Bistolas, U. Wollenberger, C. Jung, F. W. Scheller, *Biosens. Bioelectron.* **2005**, *20*, 2408–2423.

[6] F. P. Guengerich, *Chem. Res. Toxicol.* **2007**, *21*, 70–83.
[7] S. Krishnan, J. B. Schenkman, J. F. Rusling, *J. Phys. Chem. B* **2011**, *115*, 8371–8380.
[8] V. V. Shumyantseva, T. V. Bulko, G. P. Kuznetsova, N. F. Samenkova, A. I. Archakov, *Biochemistry* **2009**, *74*, 438–444.
[9] N. Sultana, J. B. Schenkman, J. F. Rusling , *JACS* **2005**, *127*, 13460–13461.
[10] Y. Mie, M. Suzuki, Y. Komatsu, *JACS* **2009**, *131*, 6646–6647.
[11] V. V. Shumyantseva, Y. D. Ivanov, N. Bistolas, F. W. Scheller, A. I. Archakov, U. Wollenberger, *Anal. Chem.* **2004**, *76*, 6046–6052.
[12] D. L. Johnson, B. C. Lewis, D. J. Elliot, J. O. Miners, L. L. Martin, *Biochem. Pharmacol.* **2005**, *69*, 1533–1541.
[13] S. Krishnan, A. Abeykoon, J. B. Schenkman, J. F. Rusling, *JACS* **2009**, *131*, 16215–16224.
[14] M. Antonini, P. Ghisellini, L. Pastorino, C. Paternolli, C. Nicolini, *IEE Proc. Nanobiotechnol.* **2003**, *150*, 31–34.
[15] C. Paternolli, M. Antonini, P. Ghisellini, C. Nicolini, *Langmuir* **2004**, *20*, 11706–11712.
[16] C. Estavillo, Z. Lu, I. Jansson, J. B. Schenkman, J. F. Rusling, *Biophys. Chem.* **2003**, *104*, 291–296.
[17] V. V. Shumyantseva, T. V. Bulko, Y. O. Rudakov, G. P. Kuznetsova, N. F. Samenkova, A. V. Lisitsa, A. I. Archakov, *Biochemistry, Moscow, Supp. Ser. B, Biomed. Chem.* **2007**, *1*, 327–333.
[18] C. Baj-Rossi, T. Rezzonico Jost, A. Cavallini, F. Grassi, G. De Micheli, S. Carrara, *Biosens. Bioelectron.* **2014**, *53*, 283–287.
[19] S. Joseph, J. F. Rusling, Y. M. Lvov, T. Friedberg, U. Fuhr, *Biochem. Pharmacol.* **2003**, *65*, 1817–1826.
[20] A. Ignaszak, N. Hendricks, T. Waryo, E. Songa, N. Jahed, R. Ngece, E. I. Iwuoha, *J. Pharm. Biomed. Anal.* **2009**, *49*, 498–501.
[21] P. M. Ndangili, A. M. Jijana, P. G. L. Baker, E. I. Iwuoha , *J. Electroanal. Chem.* **2011**, *653*, 67–74.
[22] V. R. Dodhia, C. Sassone, A. Fantuzzi, G. D. Nardo, S. J. Sadeghi, G. Gilardi, *Electrochem Commun.* **2008**, *10*, 1744–1747.
[23] G. R. Harlow, J. R. Halpert, *J. Biol. Chem.* **1997**, *272*, 5396–5402.
[24] G. R. Harlow, J. R. Halpert, *PNAS*, **1998**, *95*, 6636–6641.
[25] T. Omura, R. Sato, *J. Biol. Chem.* **1964**, *239*, 2379–2385.
[26] A. L. Shen, T. D. Porter, T. E. Wilson, C. B. Kasper, *J. Biol. Chem.* **1989**, *264*, 7584–7589.
[27] D. R. Davydov, E. Deprez, G. H. B. Hoa, T. V. Knyushko, G. P. Kuznetsova, Y. M. Koen, A. I. Archakov, *Arch. Biochem. Biophys.* **1995**, *320*, 330–344.
[28] S. Carrara, V. V. Shumyantseva, A. I. Archakov, B. Samorí, *Biosens. Bioelectron.* **2008**, *24*, 148–150.
[29] S. Carrara, A. Cavallini, V. Erokhin, G. De Micheli, *Biosens. Bioelectron.* **2011**, *26*, 3914–3919.
[30] S. Carrara, A. Cavallini, A. Garg, G. De Micheli, *ICME Int. Conf.* **2009**, 1–6.
[31] C. Baj-Rossi, G. De Micheli, S. Carrara, *Sensors* **2012**, *12*, 6520–6537.
[32] J. Mocak, A. M. Bond, S. Mitchell, G. Scollary, *Pure Appl. Chem.* **1997**, *69*, 297–328.
[33] J. N. Miller, J. C. Miller, *Statistics, Chemometrics for Analytical Chemistry,* 6th ed., Prentice Hall, Harlow, UK, **2005**.
[34] A. Shukla, E. M. J. Gillam, P. V. Bernhardt, *Electrochem Commun.* **2006**, *8*, 1845–1849.
[35] L. Zhao, H. Liu, N. Hu, *J. Colloid Interf. Sci.* **2006**, *296*, 204–211.
[36] M. Wirtz, V. Oganesyan, X. Zhang, J. Studer, M. Rivera, *Faraday Discuss.* **2000**, *116*, 221–234.
[37] C. Cai, J. Chen, *Anal. Biochem.* **2004**, *325*, 285–292.
[38] N. C. Veitch, *Phytochemistry* **2004**, *65*, 249–259.
[39] A. J. Bard, L. R. Faulkner, *Electrochemical Methods,* 5th ed, Wiley, New York, **1980**.
[40] H. Liu, N. Hu, *Anal. Chim. Acta* **2003**, *481*, 91–99.
[41] J. Wang, *Electroanalysis* **2004**, *17*, 7–14.
[42] A. J. Ahammad, J. J. Lee, A. Rahman, *Sensors* **2009**, *9*, 2289–2319.
[43] Q. Zhao, Z. Gan, Q. Zhuang, *Electroanalysis* **2002**, *14*, 1609–1613.
[44] M. Anttila, M. Haataja, A. Kasanen, *Eur. J. Clin. Pharmacol.* **1980**, *18*, 263–268.
[45] Z. Huang, P. Roy, D. J. Waxman, *Biochem. Pharmacol.* **2000**, *59*, 961–972.
[46] J. M. Singer, J. M. Hartley, C. Brennan, P. W. Nicholson, R. L. Souhami, *Br. J. Cancer* **1998**, *77*, 978.
[47] R. A. Upton, R. L. Williams, J. Kelly, R. M. Jones, *Br. J. Clin. Pharmacol.* **1984**, *18*, 207–214.
[48] S. Liu, L. Peng, X. Yang, Y. Wu, L. He, *Anal. Biochem.* **2008**, *375*, 209–216.
[49] E. Iwuoha, R. Ngece, M. Klink, P. Baker, *IET Nanobiotechnol.* **2007**, *1*, 62–67.
[50] P. A. Boudreau, S. P. Perone, *Anal. Chem.* **1979**, *51*, 811–817.
[51] J. J. Toman, S. D. Brown, *Anal. Chem.* **1981**, *53*, 1497–1504.
[52] S. V. Romanenko, A. G. Stromberg, T. N. Pushkareva, *Anal. Chim Acta* **2006**, *580*, 99–106.

Received: December 15, 2014
Accepted: January 12, 2015
Published online: March 24, 2015

